Langmuir

Letter

pubs.acs.org/Langmuir

Toward Nanoscale Three-Dimensional Printing: Nanowalls Built of Electrospun Nanofibers

Minhee Lee and Ho-Young Kim*

Department of Mechanical and Aerospace Engineering, Seoul National University, Seoul 151-744, Korea

ABSTRACT: Although the extreme miniaturization of components in integrated circuits and biochemical chips has driven the development of various nanofabrication technologies, the 3D fabrication of nanoscale objects is still in its infancy. Here we propose a novel method to fabricate a free-standing nanowall by the precise, repetitive deposition of electrospun polymer nanofibers. We show that the electrified nanojet, which tends to become unstable when traveling in air because of coulombic repulsion, can be stably focused onto the microline of a metal electrode. On the conducting line, the polymer nanojet is spontaneously stacked successively to form a wall-like structure. We rationalize the length of the wall by balancing the tension in the polymer fiber with the electrostatic interaction of the fiber with the metal ground. We also show that the length of a nanowall can be controlled by translating the substrate. This novel 3D printing scheme can be applied to the development of various 3D nanoscale objects including bioscaffolds, nanofilters, nanorobots, and nanoelectrodes.

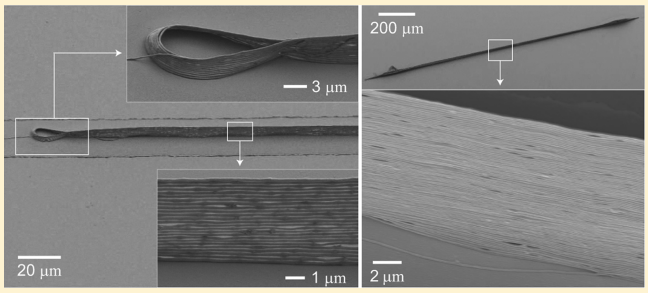

INTRODUCTION

The fabrication of 3D objects through the direct deposition of functional materials has been a subject of intense study in the area of macroscale manufacturing for several decades.[1] So-called 3D printing is reaching a stage where the desired products can be made independently of the complexity of their shapes, thus drawing a great amount of attention as a promising manufacturing technology that is fast, less wasteful, and economically viable.[2] Applying such a concept to nanofabrication technology can bring about similar advantages. In addition, prepatterned nanostructures or microstructures can be used as substrates, and thus unprecedented manufacturing flexibility, functionality, and complexity can be realized on the nanoscale.

Examples of direct deposition processes on the nanoscale include dip-pen nanolithography (DPN), which draws a collection of molecules into lines with widths of tens of nanometers,[3] and inkjet printing, which deposits discrete droplets with diameters in the micrometer range.[4] However, their capability of producing 3D nanoscale objects has not been demonstrated yet. DPN needs extreme accuracy in alignment to deposit molecules on top of their predeposit. Also, it is very hard to control the meniscus shape and the diffusion rate of target molecules contained in the limited volume of solvent because the solvent tends to evaporate and spread over the substrate rather than stack on itself. The deposition of inks that are injected through nozzles of tens of micrometers of diameter and then solidified has been successfully used to create a variety of submillimetric devices,[5,6] but a size limitation exists that prevents the fabrication of nanoscale objects.

Electrojetting is an attractive and viable process to deposit nanoscale objects, which uses nanofibers emitted from a liquid droplet under a strong electrical field.[7] Major difficulties of utilizing electrojetting for nanofabrication come from the intrinsic instability of electrified nanojets experiencing mutual coulombic repulsion.[8] Chaotic piles of nanofibers were used for 3D fabrication in which the feature sizes ranged from the order of 0.1 to 1 mm.[9,10] Although there were attempts to collect individual nanofibers by placing the substrate near the source of the nanojet before the instability sets in[11] or using collectors with a very fine gap over which nanofibers were suspended,[12] the objects made through these methods are only 2D. Three-dimensional meshes were built by individual electrospun fibers produced by melt electrospinnig,[13] but the constituent fiber's diameter was a few micrometers because the melt viscosity needed to be high enough to slow the jet velocity. It was shown that a nanoscale electrojet can coil to form free-standing pottery because the jet is focused onto a sharp electrode tip, but this method is limited to fabricating hollow cylindrical structures.[14]

Here, we present a novel method to create 3D nanostructures using nanofibers produced by electrospinning. To control the whipping instability of the electrical nanojets, we use a conducting microline on an insulating plate as a ground that focuses the electrical field. To stack the fibers in a controlled fashion, we manipulate the fiber deposit into attracting the incoming nanojets rather than repelling them by draining the electrical charge quickly. Then we get a nanowall that lines the ground, implying that various free-standing structures can be created by patterning the microscale ground lines in a desired shape. In the following section, we detail the processing

Received: December 7, 2013
Revised: January 28, 2014
Published: January 28, 2014

   dx.doi.org/10.1021/la404704z | *Langmuir* 2014, 30, 1210−1214

conditions used to realize this novel fabrication scheme and report the observations of the resulting nanostructures. Also, we elucidate the fundamental electromechanical mechanism that enables the spontaneous stacking of a nanofiber onto itself to provide a physical basis behind this novel nanofabrication process.

EXPERIMENTAL SECTION

Figure 1 shows the experimental apparatus consisting of a syringe pump that supplies a 10 wt % aqueous polymer solution of poly(ethylene oxide) (PEO, viscosity-average molecular weight 300 000 g/mol) to a metal capillary of 100 μm inner diameter, a glass ground plate situated 3 mm from the drop hanging from a capillary, a high-voltage source, and a high-speed camera. Any polymer solution whose fiber evaporates fast enough to prevent its deposit from reflowing can be used for this process. The flow rate of the polymer solution through the capillary is set to be approximately 5 μL/h, and the nanojet starts to be emitted with a speed of about 50 mm/s from a drop of 200 μm diameter at an electrical field strength of 1.2 kV/mm. Once the jet is issued, the electrical field is reduced to 0.5 kV/mm to decrease the jet speed to below 40 mm/s. When a metal plate is used as a ground, the resulting deposit is a chaotic pile of nanothreads as shown in Figure 2a. This is due to the instability of the electrical jet typical of the system employing a conducting ground plate that tends to spread out the electrical field lines as illustrated in Figure 2b. To focus the jet, we deposit a platinum line of 20 μm width on the glass plate by the sputtering and lift-off process. The microscopic ground effectively focuses the electrical field as shown in Figure 2c and consequently the electrical jet.

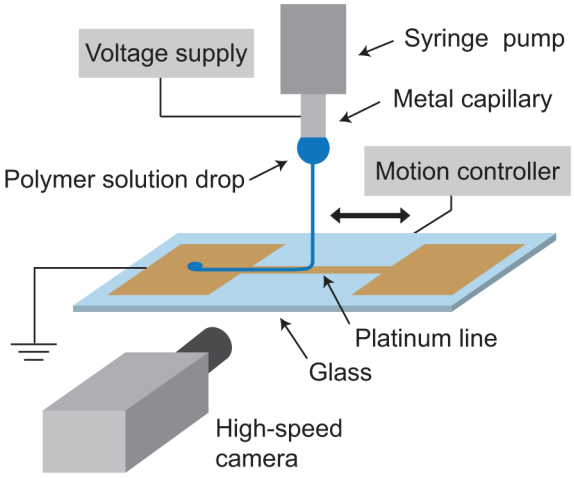

Figure 1. Schematic of the experimental apparatus.

RESULTS AND DISCUSSION

Fabrication of Nanowalls on a Stationary Substrate. We first present the results of depositing nanofibers on a stationary, straight-line platinum ground. Figure 3a,b shows the dynamic behavior of a nanojet impinging on a straight platinum line. The high voltage on the drop and consequently the high-density surface charges on the drop and nanofibers induce the opposite charges on the adjacent ground plate. The induced charges tend to gather on the conducting metal line rather than on the insulating glass plate. Therefore, the nanojet is strongly attracted to the metal line. Once impinging on the ground, the nanojet bends to touch the oppositely charged metal line, thereby forming a nanoline. When the angle between the line vertical to the plate and the bent jet, α, reaches a limit, α_m, the jet turns as shown in Figure 3b. The nanothread loses its charges as it contacts the metal ground and then attains a charge of the opposite polarity to attract the following nanojet. Then the nanojet is piled precisely on top of the predeposited nanothread until it reverses its direction at $\alpha = -\alpha_m$. This process is repeated, the consequence being a free-standing nanowall consisting of the precisely stacked nanothreads as shown in Figure 3c. We used a nanojet of 180 nm diameter and 30 mm/s velocity to construct the 4.5-μm-tall, 220-μm-long nanowall in Figure 3c. The oscillation frequency of the nanojet was 68 Hz, implying that it took 0.18 s to stack 25 lines.

Observing the ends of the nanowall (Figure 3d) reveals that the nanojet forms a racket as it turns at $\alpha = \pm\alpha_m$. Although the jet first deviates from the xy plane (indicated in Figure 3b) at α_m, it is pushed back to the xy plane owing to the electrostatic focusing effect that increases with the deviation distance from the xy plane. As illustrated in Figure 3e, the jet in Figure 3d first rotates clockwise because of a small perturbation but soon bends counterclockwise to make a full circle as a result of the electrostatic focusing effect.

Estimation of Nanowall Length. To estimate the maximum angle that the nanojet can form with respect to the vertical before turning, which determines the length of the spontaneously formed nanowall, we consider the torques acting on the curved segment of the jet near the substrate (Figure 3b). As the jet angle α increases, the horizontal component of the tension T in the jet arising from the electrostatic attraction from the ground line, $T_h = T \sin \alpha$, increases. This horizontal force component makes the jet prone to rotation because of a small perturbation from the xy plane, designated as δ in Figure 3b, so that the jet could turn back. The tendency to deviate from the xy plane is suppressed by the strong focusing effects of the narrow metal line for small α. However, as α increases, the torque induced by the horizontal force, $T_h\delta$, increases. As soon as this destabilizing torque overcomes the stabilizing torque, the jet turns.

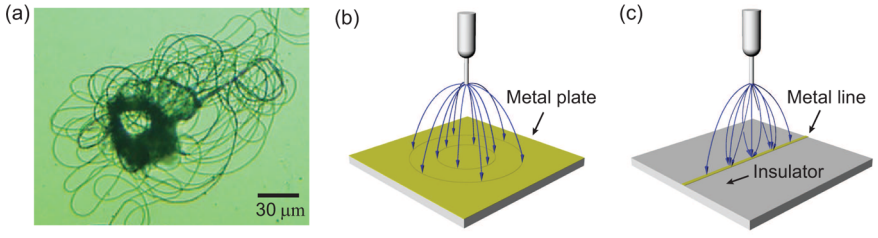

Figure 2. Effects of the electric field distribution on the deposition of a nanofiber. (a) Chaotic pile of nanothreads on a platinum plate ground. Schematics of electric field distribution on (b) a plate ground and (c) a line ground on an insulating plate.

dx.doi.org/10.1021/la404704z | Langmuir 2014, 30, 1210−1214

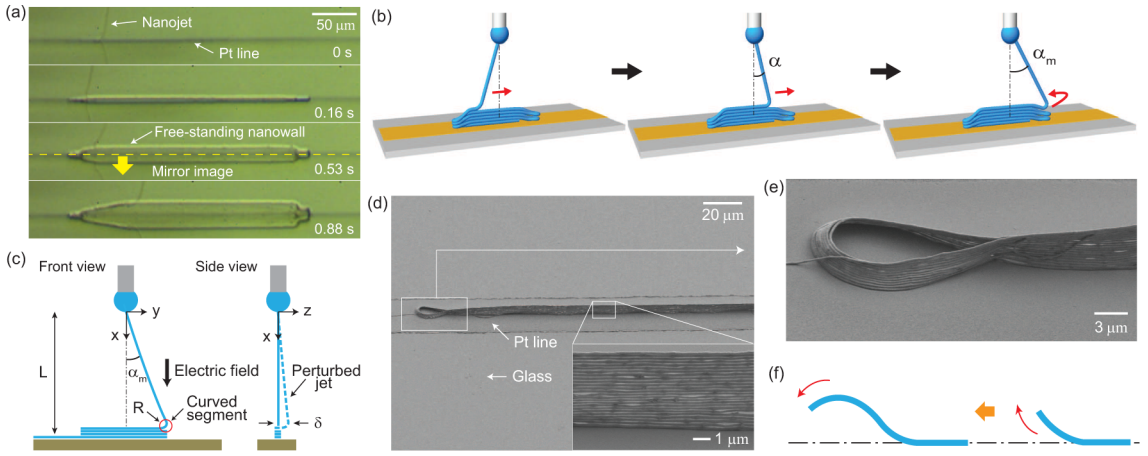

Figure 3. Nanowall built on a stationary metal line. (a) High-speed sequential images of a nanojet constructing a nanowall through spontaneous oscillation and stacking. (b) Illustration of the deposition of a nanofiber to yield a free-standing nanowall. (c) Schematic of a nanojet that is about to turn because of lateral perturbation that cannot be stabilized as the bending angle α reaches α_m. (d) SEM (scanning electron microscopy) images of the free-standing nanowall. (e) SEM image of the end of the nanowall that resembles a racket. (f) Trajectory of the jet-impinging point during a turn.

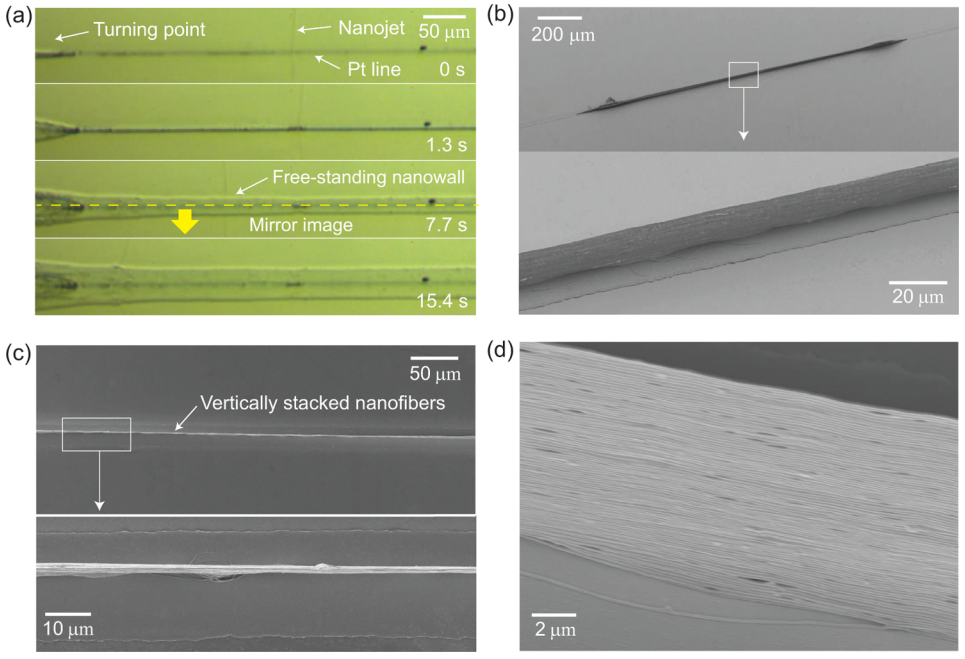

Figure 4. Long nanowall built on a translating metal line. (a) High-speed sequential images of a nanojet constructing a 1-mm-long nanowall. (b) Tilted view of the nanowall. Local peaks appear at the ends because the substrate needs to stop to reverse its direction. (c) Top view verifying that the nanowall stands vertical to the metal line. (d) Magnified tilted view of the nanowall showing that 98 nanothreads of 180 nm diameter have been stacked precisely on top of the predeposited thread.

The stabilizing torque is scaled as F_eR with the lateral electrostatic focusing force of $F_e \approx 2\pi qrRE_t$, where q, r, and R are the surface charge density, the radius of the jet, and the radius of curvature of the nanojet near the impinging point, respectively. E_t, the transverse electric field (in the z direction in Figure 3b) established near the substrate as a result of the finite width of the metal line, depends on δ and the vertical electrical field intensity. The symbol "≈" signifies "is scaled as". Utilizing the electrical field distribution around a finite line charge,[15] the transverse and vertical electric fields near the substrate can be approximated as $E_t \approx Q\delta/w^3$ and $E_v \approx Q/(wR)$, respectively. Here, Q is the charge on the conducting line, and w is half of the line width. E_v can be estimated using the vertical electrical field between the drop and the ground, E, so that $E_v \approx E \approx V/L$, where V is the voltage applied at the drop and L is the distance between the drop and the ground. E_t is related to E as $E_t \approx ER\delta/w^2$. The surface charge density of a conducting object charged by external electrical field E, q_0, is given by $q_0 \approx \varepsilon_0 E$, where ε_0 is the vacuum permittivity.[16] However, for a nanojet emitted from a macroscale drop, the surface charge density q is known to be approximately 2 orders of magnitude higher than q_0.[17,18] This is because the electrical field intensity is locally magnified where the drop is stretched severely to issue a jet so that the bulk conduction decreases while the surface convection increases.[18,19] Thus, we write $q \approx a\varepsilon_0 E$, with a being the magnification factor of the surface charge, $a \approx 10^1-10^2$. Balancing the two torques, $T_h\delta$ and F_eR, in opposite directions gives $\sin \alpha_m \approx 2\pi a\varepsilon_0 rE^2R^3/(w^2T)$.

dx.doi.org/10.1021/la404704z | Langmuir 2014, 30, 1210−1214

The tension of the jet, which is effectively a solid by the time it impinges on the target as a result of the evaporation of the solvent during flight,[14] is directly related to the curvature of the jet bent near the substrate. It is determined by a balance between the torque due to the electrostatic tension $TR \cos \alpha_m$ and the elastic torque YI/R, where Y is Young's modulus of the fiber and I is the area moment of inertia ($I = r^4/12$).[14] Thus, we get $T \approx YI/(R^2 \cos \alpha_m)$, which yields the maximum jet bending angle α_m as $\tan \alpha_m \approx 24\pi a\varepsilon_0 E^2 R^5/(Yr^3w^2)$.

The magnification factor of the surface charge, a, for the nanojet can be estimated from the results of the experiments that used the same type of nanojet as used in this work. Kim et al.[14] showed that a nanojet of PEO solution under the same voltage condition impinging on a sharp ground tip, rather than the electrode line as used here, coils to form a hollow cylindrical structure (i.e., nanopottery). The coil radius, R_c, was shown to be scaled as $R_c \approx 0.21[Y/(24\pi\varepsilon_0 E^2)]^{1/3} r$, where the proportionality constant 0.21 was experimentally determined. By introducing the factor a into the model, we get $R_c \approx k[Y/(24\pi a\varepsilon_0 E^2)]^{1/3} r$, where $a = 106$ makes the proportionality constant k unity. Therefore, we see that the magnification factor a of our system lies in the same range as previously predicted.[17,18]

Because the radius of curvature of the nanofiber as it impinges on the ground line, R, and the radius of the pottery, R_c, are determined by the same torque balance, we get $R \approx R_c$, which finally gives the scaling law for the maximum jet bending angle, α_m:

$$\tan \alpha_m \approx \left(\frac{Y}{24\pi a\varepsilon_0 E^2}\right)^{2/3} \frac{r^2}{w^2} \quad (1)$$

This implies that a longer nanowall is obtained as the jet gets thicker and stiffer (large r and Y) and the electrical field gets weaker and the ground line becomes narrower. Using the experimental conditions $E = 5 \times 10^5$ V/m, $Y = 0.4$ GPa,[14] $r = 100$ nm, and $w = 10$ μm, we get $\alpha_m \approx 5°$. This value is of the same order of magnitude as our experimental measurement, $\alpha_m = \tan^{-1}(l/L) = 2°$ with $L = 3$ mm and half of the wall length being $l = 0.11$ mm. The actual jet bends more as it approaches the substrate because of the electrostatic forces, just as a catenary in the gravitational field,[20] implying an increased value of α_m compared to $\tan^{-1}(l/L) = 2°$.

Fabrication of Nanowalls on a Moving Substrate. The range of wall length that can be achieved by the spontaneous piling and turning of nanothreads is rather limited. Thus, in this section we employ the motion of the substrate to control the length of nanowalls. Figure 4a shows the time sequence of nanowall construction by translating the substrate in the direction of the metal line with a stroke of 1 mm. The speed of the substrate must be set approximately equal to the incoming speed of the jet so that the angle between the jet and the substrate can be maintained at approximately 90°. If the substrate speed is less than that of the jet, then the jet oscillates as if it were being deposited on the foregoing stationary substrate. Thus, multiple layers of different lengths are deposited when the substrate travels once from one end to the other. For a substrate speed greater than that of the jet, the jet is severely stretched as the impinging point moves away from the center line. Then the jet can either be cut or turn before the substrate makes a full stroke. Figure 4b–d shows SEM images of the 1-mm-long nanowalls built by translating the substrate at 40 mm/s, which matches the speed of the jet. Figure 4a,b shows that the wall height exhibits a local peak at the ends where the substrate speed becomes zero as the translational direction is reversed. The jet turns locally as if it were impinging on a stationary plate in this region, thereby forming thick shoulders. The ratio of the length of the wall shown in Figure 4b (1 mm) to the thickness (180 nm) is 5.6×10^3, and that of the height to the thickness is approximately 100. We succeeded in stacking up to 300 nanothreads vertically using the reciprocating linear stage. The stability of the nanowall, or the maximum height of the nanowall achievable via the current process, increases with the increase in wall length owing to a longer time for charge release and the decrease in the metal line width owing to increased field-focusing effects.

■ CONCLUSIONS

We have shown that nanoscale 3D objects such as free-standing nanowalls can be constructed as an electrospun polymer solution jet is focused onto a thin metal electrode line. Even without the motion of the substrate, nanojets are spontaneously laid down and piled to yield nanowalls. A scaling law that captures the essential physics behind the turning of a nanofiber allows us to estimate the length of the nanowall and also to think about controlling the wall geometry using experimental parameters. This current process needs only a power supply and a linear stage to build free-standing nanowalls after drawing metal microlines, all of which can be conducted under normal laboratory conditions. Therefore, it has a significant economic advantage as compared to conventional nanomanufacturing processes used to build nanowalls such as DRIE (deep reactive ion etching). In particular, the current scheme of repeatedly stacking fibers on a conducting line is suited for fabricating nanoelectrodes consisting of straight walls[6] and nanochannel FETs (field effect transistors) utilizing insulating nanowalls as gaps in metal patterns.[21]

Furthermore, combining the motion of the substrate and the prepatterning of microscale electrodes has the potential to build nanostructures of complicated shapes. Challenges to overcome in the future to attain this end include enabling the nanofiber to turn sharp corners of prepatterned ground lines.[22,23] Although simply lowering the jet speed can enable the fiber to follow complicated pattern shapes as demonstrated with microscale fibers by Brown et al.,[13] more sophisticated methods of manipulating electrical field lines, such as electrostatic or magnetic deflectors that were used for cathode ray tubes[24] and quadrupole ion traps for mass spectrometry,[25] have the potential to realize the rapid 3D printing of complicated shapes, which can be used for bioscaffolds, nanofilters, and nanorobots.

■ AUTHOR INFORMATION

Corresponding Author

*E-mail: hyk@snu.ac.kr. Phone: +82 (0)2 8809286. Fax: +82 (0)2 8809287.

Notes

The authors declare no competing financial interest.

■ ACKNOWLEDGMENTS

This work was supported by the National Research Foundation of Korea (grant nos. 2011-0030744 and 2013034978) via SNU-IAMD.

REFERENCES

(1) Sachs, E. M.; Cima, M. J.; Williams, P.; Brancazio, D.; Cornie, J. Three-dimensional printing: rapid tooling and prototypes directly from a CAD model. *J. Eng. Ind.* **1992**, *114*, 481−488.

(2) Bird, J. Exploring the 3D printing opportunity. *Financ. Times*; August 8, **2012**.

(3) Piner, R. D.; Zhu, J.; Xu, F.; Hong, S.; Mirkin, C. A. Dip-pen nanolithography. *Science* **1999**, *283*, 661−663.

(4) Sirringhaus, H.; Kawase, T.; Friend, R. H.; Shimoda, T.; Inbasekaran, M.; Wu, W.; Woo, E. P. High-resolution inkjet printing of all-polymer transistor circuits. *Science* **2000**, *290*, 2123−2126.

(5) Gratson, G. M.; Xu, M.; Lewis, J. A. Direct writing of three-dimensional webs. *Nature* **2004**, *428*, 386.

(6) Sun, K.; Wei, T.-S.; Ahn, B. Y.; Seo, J. Y.; Dillon, S. J.; Lewis, J. A. 3D printing of interdigitated Li-ion microbattery architectures. *Adv. Mater.* **2013**, *25*, 4539−4543.

(7) Reneker, D. H.; Yarin, A. L. Electrospinning jets and polymer nanofibers. *Polymer* **2008**, *49*, 2387−2425.

(8) Reneker, D. H.; Yarin, A. L.; Fong, H.; Koombhongse, S. Bending instability of electrically charged liquid jets of polymer solutions in electrospinning. *J. Appl. Phys.* **2000**, *87*, 4531−4547.

(9) Zhang, D.; Chang, J. Eletrospinning of three-dimensional nanofibrous tubes with controllable architectures. *Nano Lett.* **2008**, *8*, 3283−3287.

(10) Bonino, C. A.; Efimenko, K.; Jeong, S. I.; Krebs, M. D.; Alsberg, E.; Khan, S. A. Three-dimensional electrospun alginate nanofiber mats via tailored charge repulsions. *Small* **2012**, *8*, 1928−1936.

(11) Sun, D.; Chang, C.; Li, S.; Lin, L. Near-field electrospinning. *Nano Lett.* **2006**, *6*, 839−842.

(12) Li, D.; Wang, Y.; Xia, Y. Electrospinning of polymeric and ceramic nanofibers as uniaxially aligned arrays. *Nano Lett.* **2003**, *3*, 1167−1171.

(13) Brown, T. D.; Dalton, P. D.; Hutmacher, D. W. Direct writing by way of melt electrospinning. *Adv. Mater.* **2011**, *23*, 5651−5657.

(14) Kim, H.-Y.; Lee, M.; Park, K. J.; Kim, S.; Mahadevan, L. Nanopottery: coiling of electrospun polymer nanofibers. *Nano Lett.* **2010**, *10*, 2138−2140.

(15) Weber, E. *Electromagnetic Fields: Theory and Applications*; Wiley: New York, 1950; p 108.

(16) Haus, H. A.; Melcher, J. R. *Electromagnetic Fields and Energy*; Prentice-Hall: Englewood Cliffs, NJ, 1989.

(17) Shin, Y. M.; Hohman, M. M.; Brenner, M. P.; Rutledge, G. C. Experimental characterization of electrospinning: the electrically forced jet and instabilities. *Polymer* **2001**, *42*, 9955−9967.

(18) Feng, J. J. The stretching of an electrified non-Newtonian jet: a model for electrospinning. *Phys. Fluids* **2002**, *14*, 3912−3926.

(19) Gañán-Calvo, A. M. On the theory of electrohydrodynamically driven capillary jets. *J. Fluid Mech.* **1997**, *335*, 165−188.

(20) Lockwood, E. H. *A Book of Curves*; Cambridge University Press: Cambridge, England, 1961; pp 118−125.

(21) Min, S.-Y.; Kim, T.-S.; Kim, B. J.; Cho, H.; Noh, Y.-Y.; Yang, H.; Cho, J. H.; Lee, T.-W. Large-scale organic nanowire lithography and electronics. *Nat. Commun.* **2013**, *4*, 1773.

(22) Li, D.; Ouyang, G.; McCann, J. T.; Xia, Y. Collecting electrospun nanofibers with patterned electrodes. *Nano Lett.* **2005**, *5*, 913−916.

(23) Luo, C. J.; Stoyanov, S. D.; Stride, E.; Pelan, E.; Edirisinghe, M. Electrospinning versus fibre production methods: from specifics to technological convergence. *Chem. Soc. Rev.* **2012**, *41*, 4708−4735.

(24) Cowley, J. M. In *Principles of Analytical Electron Microscopy*; Joy, D. C., Romig, A. D., Jr., Goldstein, J. I., Eds.; Plenum: New York, 1986; pp 77−120.

(25) Todd, J. F. J.; March, R. E. *Quadrupole Ion Trap Mass Spectrometry*; Wiley: Hoboken, NJ, 2005.

MOLECULAR BIOLOGY

How proteins find their DNA target

Researchers have captured images of individual proteins searching for their DNA-binding sites, and have quantified parts of this process.

Zhe Liu and his team at the Howard Hughes Medical Institute in Ashburn, Virginia, looked at transcription factors — proteins that bind to specific genes to regulate their activity — in individual, living mouse embryonic stem cells. The researchers used microscopes to track single molecules of Sox2 and Oct4, key stem-cell gene regulators. They found that the two molecules use trial and error to seek out their binding sites, by colliding with DNA, diffusing away and colliding again roughly 90 times before finding their targets. The process takes about 6 minutes and the factors remain bound to the target sites for about 12 to 14 seconds.

Sox2 collides and then slides along short stretches of DNA. Sox2 also binds before Oct4, helping it to find its home.

Cell 156, **1274–1285 (2014)**

PHRED PETERSEN/SHIYANG TANG/RMIT

GLACIOLOGY

More of Greenland is starting to melt

Once-stable glaciers in northeast Greenland are now shrinking as a result of regional warming.

Shfaqat Khan at the Technical University of Denmark in Kongens Lyngby and his colleagues analysed satellite and airborne-elevation measurements of three glaciers that comprise the 600-kilometre-long northeast Greenland ice stream. The measurements revealed that, after more than a quarter of a century of stability, this stream began to thin between 2003 and 2006. The team then looked at ocean and atmospheric temperature data and determined that warmer air temperatures, beginning in 2003, probably led to the melting of sea ice in the region, allowing the glaciers to flow more freely into the ocean.

These ice-loss measurements exceed projections made for this region, and so models of global sea-level rise may underestimate Greenland's contribution over the coming century.

Nature Clim. Change **http://doi.org/rxb (2014)**

AGRICULTURE

Warming climate threatens crops

Climate change could result in decreasing yields of staple food crops in most parts of the world from the 2030s onwards.

Andrew Challinor at the University of Leeds, UK, and his team compared the results of more than 1,700 simulations of climate change impacts — with and without various adaptation strategies — on annual wheat, rice and maize (corn) yields. The data suggest that, without adaptation, average food-crop supplies will decline by around 5% per degree Celsius of warming.

Losses of wheat in temperate climates and rice in tropical environments can be avoided, or even reversed, by changing factors such as crop varieties, planting time, fertilizer use and irrigation. But such adaptation measures may provide little or no benefit for maize yields, particularly in tropical regions, the authors warn.

Nature Clim. Change **http://doi.org/rw9 (2014)**

HUMAN EVOLUTION

Hominin explorers were poor planners

Hominin migrations, such as those out of Africa, might have been led by indivduals with low levels of foresight.

A team led by Colin Wren at McGill University in Montreal, Canada, modelled the migratory behaviour of individuals, based on the complexity of their environments and their cognitive ability to assess and seek out better environments.

The model predicted that those with poorer foresight were more likely to stumble on a better habitat, and therefore disperse into new areas. Furthermore, homogeneous environments fostered exploration because the more constant level of resources allowed explorers to travel further than those in a more heterogeneous setting.

J. Hum. Evol. **http://doi.org/rwd (2014)**

PHYSICS

Micro-pump with no moving parts

A pump can propel liquids along millimetre-sized channels at high speeds with no mechanical parts.

The pump, designed by Khashayar Khoshmanesh at the Royal Melbourne Institute of Technology University in Australia and his colleagues, is a droplet of metal — an alloy of gallium, indium and tin — that is held loosely in a spherical chamber in the middle of a Plexiglas channel. A slow chemical reaction in the metal droplet results in gallate anions diffusing to the droplet's surface. When a low-power electric field is applied, the rearrangement of charges at the droplet's surface causes it to shift in its constrained space in such a way that the surrounding solution flows past it (**pictured**).

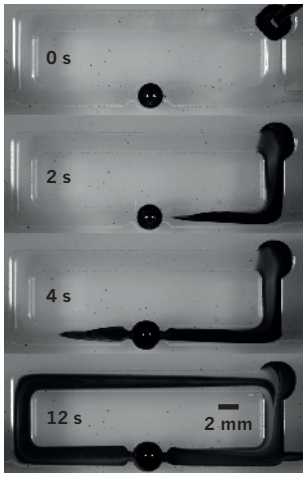

The pump might be useful in microscopic machines, the researchers say.

Proc. Natl Acad. Sci. USA 111, **3304–3309 (2014)**

COMMUNITY CHOICE

The most viewed papers in science

NANOTECHNOLOGY

3D printing goes nanoscale

HIGHLY READ on pubs.acs.org in February

Researchers have used a three-dimensional (3D) printing technique to stack nanometre-scale polymer threads on top of one another, forming a tiny wall.

A promising 3D nanoscale printing method involves spinning nanofibres out of a liquid under a strong electrical field. But only certain shapes have been printed this way, because the fibres tend to electrically repel each other. To solve this problem, Minhee Lee and Ho-Young Kim of Seoul National University fired polymer nanofibres onto a metal template sitting on top of a grounding plate that quickly drains the deposited fibres of charge. The fibres then spontaneously attract each other, and stack to form a free-standing wall.

The technique cannot yet be used to print objects with sharp corners but could still be useful for building, for example, tiny transistors, the authors say.

Langmuir 30, **1210–1214 (2014)**

NATURE.COM

For the latest research published by *Nature* visit:
www.nature.com/latestresearch